Spin polarized current in graphene pumped by a THz-signal

Aziz N. Mina[1], Adel H. Phillips[2]

[1]Faculty of Science, Beni-Suef University, Beni-Suef, Egypt
[2]Faculty of Engineering, Ain-Shams University, Cairo, Egypt
Email: phillips_adel@yahoo.com and azizmina55@yahoo.com

Abstract

Spin polarized transport properties of the Dirac electrons through ballistic mesoscopic device is investigated. This mesoscopic device is modeled as ferromagnetic graphene/ superconducting graphene junction. The transport of electrons through such junction is studied under the effect of both magnetic field and the energy of the induced photons of an AC-field. Both the Andreev and normal reflections probabilities are deduced by solving Dirac-Bogoliubov-deGennes equation analytically. The present results show an oscillatory behavior of the conductance for parallel and anti-parallel spin alignment. These oscillations are due to Fano resonance. Results for spin polarization and giant magneto-resistance show the coherency manipulation of the spin precession in such mesoscopic device. The present results are very important for quantum information processing and quantum computing and for the realization of graphene based nanoelectronics for high frequency applications.

Keywords: Ferromagnetic Graphene, Superconducting Graphene, AC-field, Spin polarization, Giant magneto-resistance, Cut-off frequency

{**Citation:** Aziz N. Mina, Adel H. Phillips. Spin polarized current in graphene pumped by a THz-signal. American Journal of Research Communication, 2013, Vol 1 (4): 100-109} www.usa-journals.com, ISSN: 2325-4076.

Introduction

It is an important issue in spintronics that how to effectively control and manipulates the spin degree of freedom in solid state systems. Since graphene exhibits high mobility, very long spin scattering time, and small spin-orbit interaction, graphene is considered as an ideal material for spin conduction [1,2]. Graphene is a single two-dimensional array of carbon atoms packed into a honeycomb lattice [3, 4]. Shubnikov-deHass oscillation measurements done on graphene show that the electrons in graphene behave like massless relativistic particles. The band structures of graphene or electronic dispersion for these particles exhibit two bands which intersect at the equivalent points K and K' [3-5]. In a 2-dimensional momentum versus E (3D) plot, the band structure appears as two cones, a right side-up cone (bottom) for the holes and an inverted cone (top) for the electrons [5,6]. The two points, K and K', are the so-called Dirac points. The cone-

like dispersion relations are similar to the energy-momentum relation for the 2D-massless relativistic particles that are governed by the 2D Dirac-Weyl equation [5-8].

Recently, graphene-superconductor hybrid systems have been investigated [9-11]. An interesting phenomenon, specular Andreev reflection (different from usual Andreev reflection) was predicted to occur the graphene-superconductor interface [9-11].

The present paper is devoted to investigate the effect of the spin-dependent specular Andreev reflections on the spin polarization of the graphene ferromagnet/ graphene superconductor junction. The spin polarization of the tunneled electrons through such junction is pumped by the influence of THz-signal.

The Model

In this section, we shall derive an expression for the conductance for the proposed spintronic device. This device is modeled as follows: ferromagnetic graphene/superconducting graphene junction which is biased by a potential, V_{sd} (See Fig.1). It is well known that the ferromagnetic graphene is a gapless graphene, while the superconducting graphene is a gapped graphene [12]. The spin polarization transport is conducted under the effect of photons of THz-field of frequency, ω, and magnetic field, B,.

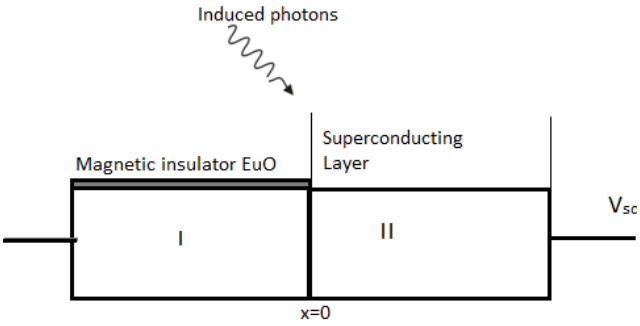

Figure 1 Region I is the ferromagnetic graphene, and region II is the superconducting graphene.

The spin transport through such junction is described by the following Dirac-Bogoliubov-deGennes equation in one dimension [12, 13].

$$\begin{pmatrix} -i\eta v_F .\sigma \partial_x - \varepsilon - \sigma h & \Delta \\ \Delta^* & i\eta v_F \sigma \partial_x + \varepsilon - \sigma h \end{pmatrix} \Psi = E\Psi \qquad (1)$$

Where v_F is the Fermi-velocity, ħ is the reduced Planck's constant, σ- Pauli matrix, h is the exchange field energy of the ferromagnetic graphene and Δ is the superconducting order parameter which is expressed in terms of its phase ϕ as:

$$\Delta = \Delta_0 e^{i\phi}, \qquad (2)$$

In Eq.(1) the parameter ε is expressed in terms of the following parameters as follows:

$$\varepsilon = E_F + eV_{sd} + eV_g + eV_{ac}\cos(\omega t) + \frac{1}{2}g\mu_B B\sigma \qquad (3)$$

where E_F is the Fermi-energy, V_{sd} is the bias voltage, V_g is the gate voltage, V_{ac} is the amplitude of the THz-field with frequency, ω, μ_B is Bohr magneton, B is the magnetic field, and g is the Lande g-factor of the ferromagnetic graphene.

The solutions of Eq.(1) are:

$$\Psi_I(x\langle 0) = \sum_{n=1}^{\infty}\left[\begin{pmatrix}1\\ e^{i\theta}\\ 0\\ 0\end{pmatrix}e^{ik_+x} + b\begin{pmatrix}1\\ -e^{-i\theta}\\ 0\\ 0\end{pmatrix}e^{-ik_+x} + a\begin{pmatrix}0\\ 0\\ 1\\ e^{-i\theta}\end{pmatrix}e^{-ik_-x}\right]J_n\left(\frac{eV_{ac}}{n\eta\omega}\right)e^{-in\omega t} \qquad (4)$$

where Ψ_I (x< 0) is the eigenfunction in the ferromagnetic graphene (region I). The eigenfunction, Ψ_{II} in the superconducting graphene (region II) is given by:

$$\Psi_{II}(x\rangle 0) = \sum_{n=1}^{\infty}\left[c\begin{pmatrix}u\\ uA_+\\ ve^{-i\phi}\\ ve^{-i\phi}A_+\end{pmatrix}e^{ik'_+x} + d\begin{pmatrix}v\\ -vA_-^*\\ ue^{-i\phi}\\ -ue^{-i\phi}A_-^*\end{pmatrix}e^{-ik'_-x}\right]J_n\left(\frac{eV_{ac}}{n\eta\omega}\right)e^{-in\omega t} \qquad (5)$$

where $k_\pm$ is the wave vector of quasiparticles in the ferromagnetic graphene (Eq.4) and is expressed as:

$$k_\pm = \frac{(E - \varepsilon \pm E_{FI})\cos\theta}{\eta v_F}, \qquad (6)$$

where E_{FI} is the Fermi-energy in the ferromagnetic graphene and θ is the Klein angle in this region I, J_n is the Bessel function of first kind, and the solutions of Eqs.(4,5) must be generated by the presence of the different side-bands "n" which come with the phase factor exp(-inωt) [15, 16]. In Eq.(4), the parameters a and b represent the spin dependent Andreev reflection and normal reflection coefficients respectively. These parameters are calculated by applying the boundary conditions at the interface of regions I & II. The wave vector $k'_\pm$ of quasiparticles in the superconducting graphene (Eq.5) and is expressed as:

$$k'_{\pm} = \frac{\left(\sqrt{\left(E_{FII} \pm \sqrt{(E-\varepsilon)^2 - \Delta^2}\right)^2 - \left(mv_F^2\right)^2}\right)\cos\theta}{\eta v_F} \tag{7}$$

where E_{FII} is the Fermi energy in the superconducting graphene (region II). For the coherence factors of electrons and holes u & v (Eq.5) are related as [14]:

$$u^2 = 1 - \mathrm{v}^2 = \frac{1}{2}\left[1 + \frac{\sqrt{E^2 - \Delta^2}}{E}\right] \tag{8}$$

The parameter A in Eq.(5) is expressed as:

$$A_{\pm} = \left(\frac{E_{FII} \pm \sqrt{\left((E-\varepsilon)^2\right) - \Delta^2} - mv_F^2}{\eta v_F k'_{\pm}}\right) e^{i\theta} \tag{9}$$

The parameter A^* (Eq.5) is the complex conjugate of A (Eq.9).

Now, applying the boundary conditions at the interface of the two regions I & II, we get the spin dependent Andreev reflection, a, and the normal reflection, b, coefficients respectively as:

$$a = \sum_{n=1}^{\infty} J_n\left(\frac{eV_{ac}}{n\eta\omega}\right) e^{-in\omega t}\left(2\cos(\theta)(A + A^*)u\,\mathrm{v}\,\mathrm{e}^{-\mathrm{i}\phi}\right) \tag{10}$$

And

$$b = \sum_{n=1}^{\infty} J_n\left(\frac{eV_{ac}}{n\eta\omega}\right) e^{-in\omega t}\left[\left(u^2 A^* + \mathrm{v}^2 A\right)2\cos(\theta) - 1\right] \tag{11}$$

The spin dependent conductance for the present investigated junction is given by [17]:

$$G_{\sigma} = \frac{4e^2}{h}\int_{E_F}^{E_F + n\eta\omega} dE\,\frac{(E_F + \varepsilon + E)W}{\pi\eta v_F}\cdot\int_0^{\pi/2} d\theta\cos(\theta)\left(1 + |a|^2 - |b|^2\right)\left(-\frac{\partial f_{FD}}{\partial E}\right) \tag{12}$$

Where W is the width of the graphene sheet and $\left(-\frac{\partial f_{FD}}{\partial E}\right)$ is the first derivative of the Fermi-Dirac distribution function which is expressed as:

$$\left(-\frac{\partial f_{FD}}{\partial E}\right)=\left(4k_BT\right)^{-1}.\cosh^{-2}\left(\frac{E-E_F+n\eta\omega}{2k_BT}\right) \quad (13)$$

in which k_B is Boltzmann constant, T is the absolute temperature and E_F is the Fermi energy in the corresponding regions of the device.

Now, the spin manipulation and detection could be achieved by determining both the spin polarization, P, and giant magnet-resistance, GMR,. These parameters are related to the conductance, G, (Eq.12), with parallel and antiparallel spin alignments through the following equations [18-20].

$$P=\frac{G_P-G_{AP}}{G_P+G_{AP}} \quad (14)$$

And

$$GMR=\frac{G_P-G_{AP}}{G_P} \quad (15)$$

where G_P is the conductance in case of parallel spin alignments and G_{AP} is the conductance in case of antiparallel spin alignments.

The cut-off frequency, υ_T, that is the frequency at which the current gain equals one. It is expressed in terms of the transconductances, $G_{m(P/AP)}$ for both parallel and antiparallel spin alignments and the total capacitances, C, of the present device as follows:

$$\nu_T=\frac{G_{m(P/AP)}}{2\pi C} \quad (16)$$

where C is the total capacitance of the graphene-based present device, given by:

$$\frac{1}{C}=\frac{1}{C_e}+\frac{1}{C_Q} \quad (17)$$

where C_e is the electrostatic capacitance and C_Q is the quantum capacitance which are given by [21]:

$$C_e=\frac{\varepsilon_{ox}}{t_{ox}} \quad (18)$$

And

$$C_Q = \frac{2e^2 k_B T}{n(\hbar v_F)^2} \ln\left[2\left(1+\cosh\left(\frac{E_F}{k_B T}\right)\right)\right] \quad (19)$$

where ε_{ox} is the dielectric constant of insulator oxide, t_{ox} is the thickness of the insulator oxide, e is the electron charge, k_B is Boltzmann constant, T is the absolute temperature, ħ is the reduced Planck's constant, v_F is the Fermi-velocity and E_F is the Fermi energy.

Results and Discussion

This section is devoted to perform numerical calculations to the conductance, G, (Eq.12) for both cases of spin alignments and also spin polarization, P, (Eq.14), giant magneto-resistance, GMR, (Eq.15) as follows:

There is a good possibility for developing novel electronic devices with graphene since it can be converted into a ferromagnetic graphene or a superconducting graphene. This can be achieved by depositing the magnetic insulator EuO on the top of the graphene; magnetic exchange energy of 5 meV can be induced into graphene sheet [18]. Also, superconducting graphene can be induced (via the proximity effect) in the graphene by placing a Aℓ/ Ti bilayer of thickness equals approximately 10 nm, on top of graphene [22]. The critical temperature, T_c. of this superconducting graphene was found to be ≅ 1.3 K [22].

So, the mesoscopic device (See Fig.1) represents the detailed structure of it as mentioned in the previous section. Numerical calculations are performed for the conductance, G, (Eq.12) for both cases of parallel and antiparallel alignment of spins. The values of the following parameters are: The width W=100 nm, temperature T=1.5K, the bias voltage V_{sd} =-1V, the exchange field energy h= 5meV, the Lande g-factor for graphene g= 4 [23] and magnetic field, B, was taken to be 0.5T. The amplitude of the induced AC-signal is V_{ac} = 0.25 V and its frequency ω≅ 10^{12}Hz (mid-infra red radiation). The Fermi energy, E_F, is calculated according to the following equation [23]:

$$E_F = \eta v_F k_F \quad (20)$$

where the value of Fermi velocity, v_F is taken to be 10^6 m/S and the Fermi wave vector, k_F, is calculated in terms of charge-carrier concentration, n , via the following equation [23]:

$$k_F = (\pi n)^{0.5} \quad (21)$$

where n≅ 0.36x10^{12} cm^{-2} [23].

It must be noted that the value of the Fermi energy, E_F, (Eq.20) must be modulated by the exchange energy of the ferromagnetic graphene (region I). Also, the value of Fermi energy, E_F, (Eq 20) must be modulated by the order parameter, Δ, of the superconducting graphene [7, 22]. The value of Δ_0 (Eq.2) might be calculated using the following equation [7, 22]:

$$2\Delta_0 = 3.53 k_B T_c \qquad (22)$$

The Klein angle, θ, was taken to be 57^0 [8]. This value was found to be optimum when computing the conductance, G, (Eq.12).

Now, the features of the present results are:

(1) Fig.2 shows the variation of the conductance, G, with the gate voltage, V_g, for both two cases of parallel and antiparallel spin alignment. An oscillatory behavior of the conductance is observed and the peak height of the resonance increases as the gate voltage increases. This oscillatory behavior, for both cases of spin alignment, might be due to Fano resonance [24]. Also, these oscillations are due to the interplay between the photon energy of the induced AC-signal and spin-up & spin down of the Cooper pairs in the superconducting graphene [22].

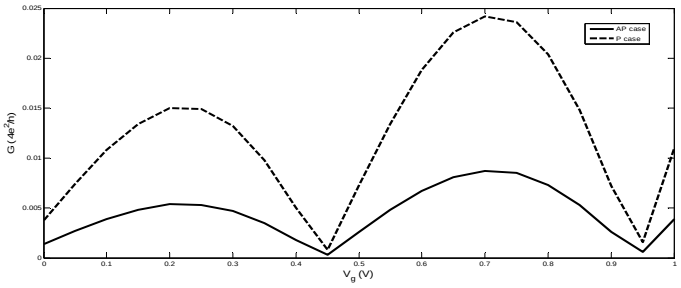

Figure 2 The variation of the conductance with the gate voltage for both cases of spin alignment

(2) Fig. 3 shows the variation of the polarization, P, with the gate voltage. This dependence is under the effect of photon energy (mid-infra red radiation). As shown from the figure, random oscillations of spin polarization are observed with random peak heights. We notice that the maximum value of the spin polarization is equal to 47.8% at V_g equals 0.25 V. While the minimum value of this spin polarization is equal to 45.5% at V_g=0.45 V.

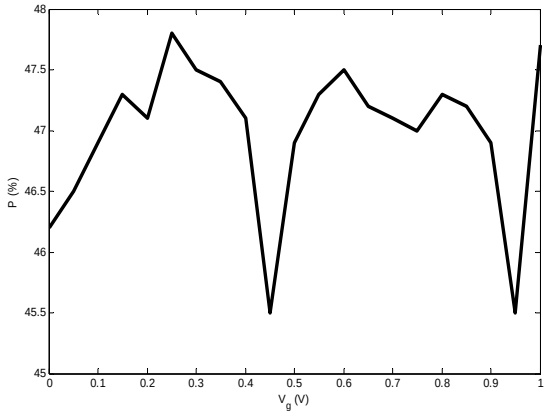

Figure 3 The variation of spin polarization, P, with the gate voltage.

(3) Fig.4. shows the variation of the giant magneto-resistance, GMR, with the gate voltage. This dependence is under the effect of photon energy (mid-infra red radiation). As shown from the figure, random oscillations of giant magneto-resistance are observed with random peak heights. We notice that the maximum value of the giant magneto-resistance is equal to 64.7% at V_g equals 0.25 V. While the minimum value of this giant magneto-resistance is equal to 62.5% at V_g=0.45 V.

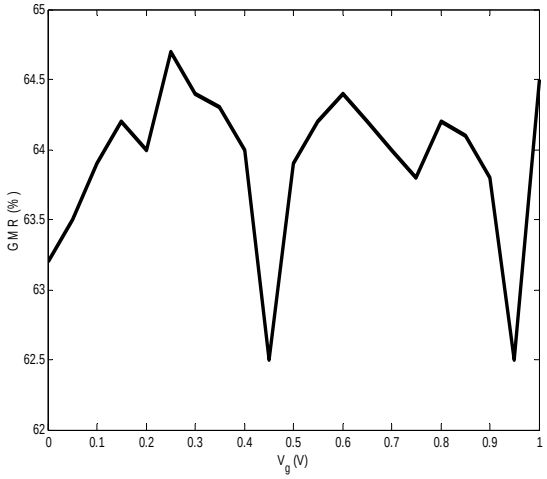

Figure 4 The variation of the giant magneto-resistance, GMR, with the gate voltage.

These random oscillations for both spin polarization, P, and giant magnet-resistance, GMR, might be due to spin flip of Dirac quasiparticles which are influenced strongly as the coupling between the induced photon energy mid-infra red radiation) and spin up & spin down subbands in the present investigated junction. Also, these oscillations might be due to the interplay between the spin-dependent specular Andreev reflection processes and spin dependent Andreev resonance process [7, 11]. The present results indicate that giant magneto-resistance might cause to raise spintronic devices which are used in read head of hard disk drives and magnetic sensors and other applications.

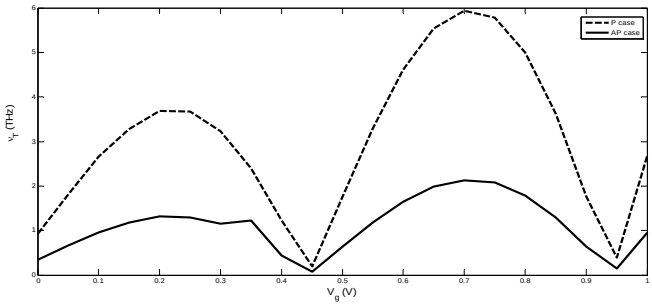

Figure 5 The variation of the cut-off frequency, υ_T, with the gate voltage, V_g, for both cases of spin alignment.

(4) Fig.5. shows the variation of the cut-off frequency, υ_T, with the gate voltage, V_g. This dependence is under the effect of induced photon energy of the applied ac-field (mid-infrared radiation). As shown from the figure, an oscillatory behavior of the cut-off frequency for both cases of spin alignment. It must be noted that in the range of the gate voltage studied the maximum values of the cut-frequency for both cases of spin alignment are, respectively,: $\upsilon_{T(P)max} = 5.93x10^{12}$ Hz at $V_g = 0.7$ V, and $\upsilon_{T(AP)max} = 2.132x10^{12}$ Hz at $V_g = 0.7V$. The present result shows that the cut-off frequency reflects the intrinsic behavior of the present studied transistor channel, where $\upsilon_{T(P/AP)max}$ also strongly might depend on device layout [25,26]. Also, the results for the cut-off frequency might be explained as follows:

According to the structure of the present investigated nano-device, the channel length is affected by the external magnetic field, that is, we must take into account the magnetic length, l_B. The second parameter is the barrier heights and the modulation of the Fermi-energy by the potential of the magnetic insulator EuO. Also, the interplay between the frequency of the induced photons with both spin-up and spin-down sub-bands plays a role in computing the cut-off frequency.

Conclusion

We conclude that the present results, for the proposed spintronic device, show that the coherent manipulation of the spin precession processes could be achieved by modulating: (a) the Fermi energy by the exchange field energy in ferromagnetic graphene (region I) and (b) the Fermi energy by the order parameter of the superconducting graphene (region II). This coherency in spin transport in the present investigated junction is fundamental issues in view of developing single spin-based quantum bits (qubits) [27] needed for quantum information processing and quantum computer.

References

1. Hill E. W., Geim A.K., Novoselov K. S., Schedin F., Blake P., (2006) IEEE Trans. Magn., 42: 2694.
2. Cheianov V. V., Fal'ko V. I., (2006) Phys. Rev. B, 74: 041403(R).
3. Novoselov K. S., Geim A. K., Morozov S. V., Jiang D., Zhang Y., Dubonos S. V., Grigorieva I. V., Firsov A. A., (2004) Science, 306**:** 666.
4. Novoselov K. S., Geim A. K., Morozov S. V., Jiang D., Katsnelson M. I., Dubonos S. V., Firsov A. A., (2005) Nature, 438: 197.
5. Castro-Neto A.H., Guinea F., Peres N. M. R., Novoselov K. S., A. K. Geim A.K., (2009) Rev. Mod. Phys., 81: 109.
6. Mina A.N., Awadallah A. A., Phillips A. H., Ahmed R. R., (2012) J. of Phys. : Conf. Series, 343, 012076.
7. Beenakker C. W. J., (2008) Rev. Mod. Phys., 80**:** 1337.
8.Mina A. N., Phillips A. H., (2011) Progress in Physics, 1: 112.
9. Beenakker C.W. J., (2006) Phys. Rev. Lett., 97**:** 067007.
10. Hsu Y. F., Guo G. Y., (2010) Phys. Rev. B, 81**:,** 045412.
11. Bai C.X., Wang J. T.,Yang Y. L., (2011) Superlattice Microstructures, 49: 151.

12. Zareyan M., Pour H. M., Maghaddam A .G.,(2008) Phys. Rev. B,78**:** 193406.
13. Bhattacharjee S.,Sengupta K., (2006) Phys. Rev. Lett., 97**:** 217001.
14. de Jang M. J. M., Beenakker C.W.J., (1995) Phys. Rev. Lett., 74: 1657.
15. Amin A.F., Li G.Q., Phillips A. H., Kleinekathofer U., (2009) Euro. Phys. J. B,68: 103.
16. Zein W. A., Ibrahim N. A., Phillips A. H., (2011)Physics Research International, 5 pages, article ID-505091.
17.Blonder G. E., Tinkham M., Klapwijk T.M., (1982) Phys. Rev. B, 25**:** 4515.
18. Haugen H., Huertas-Hernando D., Brataas A.,(2008) Phys. Rev. B,77**:** 115406.
19.Yokoyama T.,(2008) Phys. Rev. B, 77**:** 073413.
20. Mojarabian F. M., Rashedi G., (2011) Physica E, 44**:** 647.
21. Fang T. , Konar A. , Xing H. , Jena D., (2007) Appl. Phys. Lett., 91**:** 092109.
22.Heersche H.B., Jarillo-Herrero P., Oostinga J. B., Vandersypen L. M. K., Morpurgo A., (2007) Nature, 446**:** 56.
23. Das Sarma S., Adam S., Hwang E. H., Rossi E.,(2011) Rev. Mod. Phys., 83: 407.
24. Miroshnickenko A. E., Flash S. , Kivshar Y., (2010) Rev. Mod. Phys., 82: 2257.
25.Wu Y., Jenkins K. A., Valdes-Garcia A., Farmer D. B., Zhu Y., Bol A. A., Dimitrakopoulos C., Zhu W., Xia F., Avouris Ph., Lin Y., (2012) Nano Lett., **12:** 3062.
26.Wu Y., Lin Y., Bol A. A.,Jenkins K. A., Xia F., Farmer D. B., Zhu Y., Avouris Ph.,(2011) Nature, 472: 74.
27. Souza F. M., Carrara T. M., Veruek E.,(2011) Phys. Rev. B, 84: 115322.